Simultaneous measurements of mobility, dispersion, and orientation of DNA during steady-field gel electrophoresis coupling a fluorescence recovery after photobleaching apparatus with a fluorescence detected linear dichroism setup

B. Tinland, L. Meistermann, and G. Weill
Institut Charles Sadron, CNRS, 6 rue Boussingault, 67083 Strasbourg, France
(Received 5 January 2000)

Orientation of molecules is responsible for the loss of separability during steady-field gel electrophoresis. In this work we develop a technique to measure simultaneously the relevant parameters involved in the separation mechanism: electrophoretic mobility, band broadening, and molecular orientation. To do that we have associated a fluorescence recovery after photobleaching (FRAP) apparatus with a fluorescence detected linear dichroism setup. This coupling allows one to follow the buildup of orientation during the FRAP experiment. Because orientation involves a change in the angular distribution of fluorescence, we have added a fluorescence polarization setup which can be used in parallel with the FRAP and gives an exact value of the steady-state orientation factor. We illustrate the possibilities of these combined experiments by analyzing the coupling of electrophoretic transport and orientation of λ DNA in 1% agarose gels.

PACS number(s): 87.15.−v, 82.45.+z, 83.10.Nn, 83.20.Fk

I. INTRODUCTION

Gel electrophoresis is the standard method for both the separation of very long double-stranded DNA and the sequencing of short single-stranded DNA fragments. Depending on the size of the fragment with respect to the pore size, Ogston sieving [1] or reptation [2] control the separation. In the reptation regime, the mobility is predicted to be inversely proportional to the DNA contour length [3]. The observed field dependence of the mobility at higher fields was originally interpreted by Lumpkin, Déjardin, and Zimm [4] using a biased reptation model (BRM), an effect resulting from the orientation of the molecule. This model was refined by Slater and Noolandi [5]; fluctuations of the terminal section of the molecule were introduced by Duke, Viovy, and Semenov [6], leading to the biased reptation model including fluctuations (BRF). Several research groups have studied the orientation of the molecules during electrophoresis. Hurley [7] has measured the steady-field orientation by fluorescence polarization anisotropy of intercalated ethidium bromide. He observed that the BRM theory does not account quantitatively for both orientation and mobility simultaneously but can separately describe either field dependence. Holzwarth and co-workers [8,9] studied the orientation by fluorescence detected dichroism of intercalated ethidium bromide and have compared the orientation and the velocity of the chain. Jonsson and Åkerman [10] have directly recorded the dichroism in the base pair uv absorption band. Mayer, Sturm, and Weill [11,12] performed a quantitative analysis of the decay of the steady-state birefringence at the end of an electric pulse. The mobility of DNA chains during electrophoresis is clearly related to the orientation of these chains. In order to study the coupling between transport and orientation of the chains, we present an experimental setup that allows us to measure at the same time the mobility, the band broadening, and the orientation of the DNA molecules migrating through a gel. From a calculation of the polarized components of fluorescence, we will show that it is possible to get a quantitative value for the orientational factor of the molecules with a fluorescent polarization technique. We illustrate the interest of simultaneous measurements of orientation and transport both in the transitory regime following the application of the field and in steady-state conditions. More extensive data on different DNAs and different agarose gels will be discussed in a forthcoming paper.

II. MATERIALS

All experiments were carried out in 0.01 *M* Tris-borate-EDTA (ethylene diamine tetra-acetic acid) buffer at *p*H 8.3 at 22 °C. Agarose is an electrophoresis grade product (ICN, Costa Mesa, CA, lot no. 59898). The gels are prepared by dissolution in boiling buffer for a few minutes; evaporated water is replaced to adjust the concentration to the initial value and the resulting stock solution is stored at 50 °C for equilibration for 1 h. We used commercial λ phage DNA (48 500 bp) from Biolabs. This solution is diluted and mixed with a solution of YOYO fluorophore (1 dye molecule for 100 bp) and then mixed with the agarose stock solution to obtain a DNA concentration much lower than the overlap concentration in solution to ensure that the molecules are moving independently of one another.

III. METHODS

A. Mobility and dispersion measurements

Measurements were carried out by a fringe pattern fluorescence bleaching technique similar to the one described by Davoust, Devaux, and Leger [13]. The light beam of an étalon-stabilized monomode argon laser ($\lambda = 488$ nm) was split and the two beams were crossed in the electrophoretic cell, providing illumination in an interference fringe pattern. The fringe spacing $i = 2\pi/q$, set by the crossing angle ϕ, ranges from 3 to 60 μm, defining the migration distance, where the scattering vector q is equal to $(4\pi/\lambda)\sin\phi/2$. All the measurements were done in the Guinier regime (qR_g

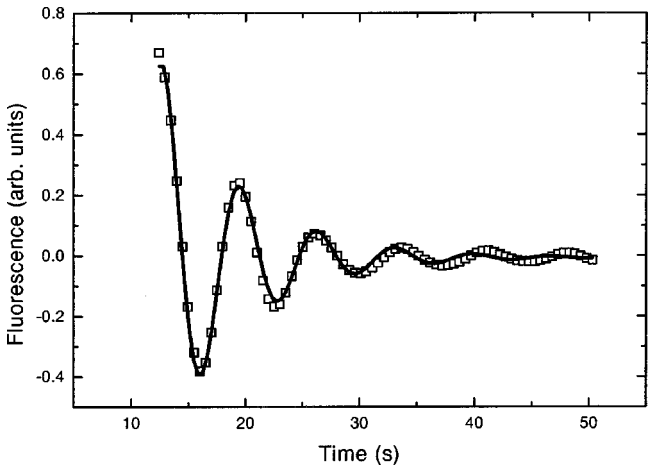

FIG. 1. Typical damped sinusoidal signal from FRAP experiment (□) fitted (continuous line) with expression (2).

≪1) ensuring that the size of the molecules is much lower than the fringe spacing. Fluorescence bleaching of the labeled polymers in the illuminated fringes was obtained by producing a 1 s full intensity bleach pulse, thus creating a fringe pattern of concentration of fluorescent molecules identical to the laser interference fringe pattern. The amplitude of the fringe pattern of concentration of fluorescent molecules was detected by modulation of the illuminating fringe position at 1 kHz using a piezoelectrically driven mirror and lock-in detection of the emerging fluorescence collected at the photomultiplier by an optical fiber. The experimental signal decays because of the band broadening, which is measured through the diffusion coefficient with electric field and spatial drift of the sample pattern.

Without electric field, in a polymer solution or gel, the diffusion of the macromolecules will lead to a monoexponential decay of the fluorescent contrast with a characteristic time τ. The self-diffusion coefficient D_s is given by

$$D_s = \frac{1}{\tau q^2}. \tag{1}$$

When the fringes are perpendicular to the field direction, the fluorescent concentration fringe pattern will move under the field, giving oscillations, and will vanish due to the band broadening. The resulting fluorescence recovery after photobleaching (FRAP) signal is a damped sinusoid (see Fig. 1) and can be fitted with the expression

$$y = A \exp\left(-\frac{t-t_0}{\tau_1}\right) \sin\left(2\pi \frac{t-t_0}{\tau_2}\right) + B. \tag{2}$$

The time τ_1, which comes from the exponential decay, corresponds under certain conditions of q (spatial drift of the sample pattern negligible compared to diffusion [14]) to the diffusion coefficient D measured in the presence of an electric field. We therefore use the name ''dispersion coefficient.'' This coefficient is given by

$$D = \frac{1}{\tau_1 q^2}. \tag{3}$$

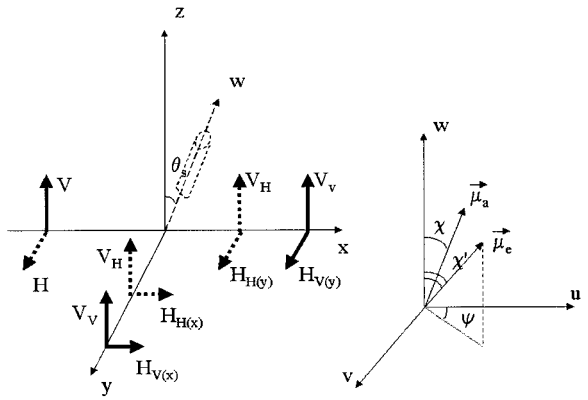

FIG. 2. Frames of reference for the calculation of the polarized components of fluorescence.

Results concerning dispersion coefficients have been reported elsewhere [15,16].

The time τ_2 is the time to cross the interfringe width i. The corresponding mobility is calculated according to

$$\mu = \frac{i}{E\tau_2}. \tag{4}$$

B. Principle of the orientation measurements

The laboratory and molecular frames of reference needed for calculation of the linear dichroism or change in fluorescence polarization due to the DNA uniaxial orientation are given in Fig. 2. Denoting by θ the angle between the absorption moment ($\vec{\mu_a}$) and Oz (the direction of the electric field taken by convention as ''vertical''), the molar absorbancies for light propagating along Ox and polarized along Oz ($\epsilon_\parallel$) or Oy ($\epsilon_\perp$) are

$$\epsilon_\parallel = \epsilon_0 \langle \cos^2 \theta \rangle, \tag{5}$$

$$\epsilon_\perp = \tfrac{1}{2} \epsilon_0 \langle \sin^2 \theta \rangle. \tag{6}$$

The linear dichroism

$$D_L = \frac{\epsilon_\parallel - \epsilon_\perp}{\epsilon_\parallel + 2\epsilon_\perp} = \frac{3\langle \cos^2 \theta \rangle - 1}{2} \tag{7}$$

can be split into

$$D_L = \frac{3\langle \cos^2 \theta_s \rangle - 1}{2} \times \frac{3\langle \cos^2 \chi \rangle - 1}{2} \tag{8}$$

when working in the absorption band of an intercalated dye with in-plane absorption $\chi = \pi/2$, and the relevant orientation factor for the calculation of a DNA segment orientation is

$$f = \frac{3\langle \cos^2 \theta_s \rangle - 1}{2} = -2D_L. \tag{9}$$

However, f does not give the mean orientation of the tube containing the DNA. It can again be split into

$$f = \frac{3\langle \cos^2 \theta_t \rangle - 1}{2} F(a/l), \tag{10}$$

where θ_t measure the orientation of the end-to-end vector of one subchain of length l in a pore of size a and $F(a/l)$ is the Kuhn and Grün factor [17], which measures the mean orientation factor of a segment with respect to the end-to-end vector $\vec{a}$ in a Gaussian chain of length l,

$$F(a/l)=1-\frac{3(a/l)}{\mathcal{L}^{-1}(a/l)} \tag{11}$$

where $\mathcal{L}^{-1}$ is the inverse Langevin function. Increase of f with the electric field therefore results from both the alignment of the tube containing the DNA (stretching) and the decrease of l or increase of the tube length (overstretching).

When using a fluorescent intercalated dye, as needed for FRAP, f can be measured from the incident polarization dependence of the total emission provided the optical density of the medium is much less than 1 [fluorescence detected linear dichroism (FDLD)]. Collecting the fluorescence in a restricted solid angle does not lead to an exact value of f since the orientation modifies the angular distribution of the fluorescence emission. It permits one, however, to follow the buildup or decay of orientation after switching on or off the electric field. It has the advantage that it can be carried out during mobility and dispersion measurements, as shown in the next section. For an exact determination of the steady-state value of f, one can use polarization of fluorescence measurements prior to the FRAP as described in Sec. III D. The advantage of using LD or polarization of fluorescence compared to birefringence is that the DNA concentration does not enter into the calculation of f.

C. The FRAP/FDLD setup

In order to measure simultaneously the mobility, dispersion, and orientation of the DNA during electrophoresis we have associated with the FRAP apparatus a fluorescence detected linear dichroism setup. The goal of this coupling is to measure μ, D, and f on the same samples in exactly the same experimental conditions. Furthermore, this coupling is less time consuming because it combines two experimental techniques. During a FDLD measurement, the difference in fluorescence intensity of the DNA–fluorescent-probe complex is observed when switching the incident light polarization between parallel (Oz) and perpendicular (Oy) directions. Neglecting the change in the anisotropy of emission, this difference is proportional to f. The experimental setup is depicted in Fig. 3. The FRAP initial setup has not been modified; the added components are represented by dotted lines. A quarter-wave plate and a photoelastic modulator modulate the polarization of light between two orthogonal directions at a frequency of 50 kHz. The fluorescence of the sample is collected by an optical fiber connected to a photomultiplier. The photomultiplier signal is analyzed by a first lock-in amplifier for detection of the ac component in phase with the polarization modulation (50 kHz). The FRAP signal is detected at the frequency of 1 kHz by a second lock-in amplifier. The signals from both lock-in detections are acquired with a microcomputer. A typical experimental signal is shown in Fig. 4. By fitting the FRAP signal (bottom of Fig. 4) with Eq. (2) we have a measure of the dispersion coefficient and of the mobility of the molecules. The FDLD buildup (top of Fig. 4) of the DNA subjected to a single

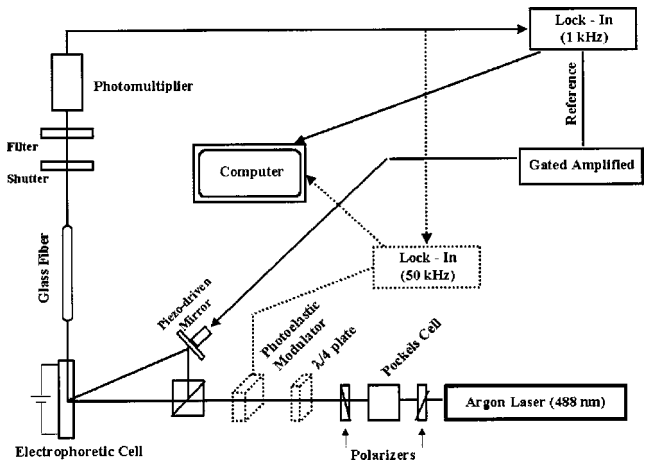

FIG. 3. Schematic diagram of the FRAP/FDLD apparatus.

electric field pulse is nonmonotonic with an overshoot and an undershoot, as already observed by several other groups [11,18,19].

D. Quantitative measurement of the orientation factor from fluorescence polarization

1. Calculation of the polarized components of fluorescence

We reduce our calculation to the components needed for the direction of emission in the plane perpendicular to the electric field taken as vertical. We follow the calculation performed by Weill and Sturm [20]. The positions of the dipole transition moments with respect to the DNA local axis w and of w with respect to the laboratory frame are specified as in Fig. 2. The four components of fluorescence resulting from vertical (V) and horizontal (H) polarizations of the incident beam are defined as V_V, V_H, H_V, and H_H where the subscript denotes the state of polarization of the incident beam and the primary letter the selected polarization of the fluorescent beam. From symmetry resulting from the uniaxial orientation in the electric field one verifies that V_V, V_H, and H_V are independent of the direction of emission in the xy plane. This is not the case for H_H. The final expressions for $\chi=\pi/2$ (intercalated dye) are

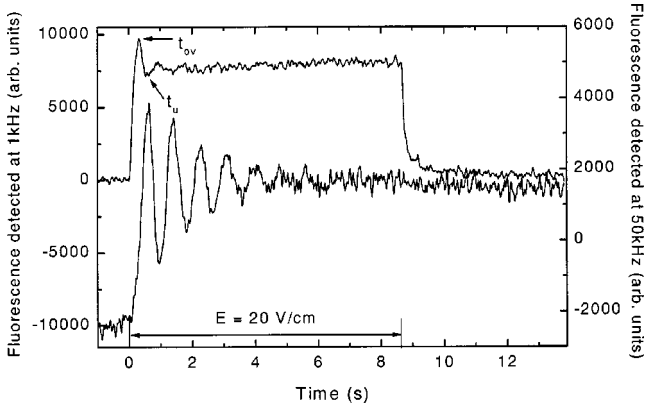

FIG. 4. Simultaneous measurement of the FRAP and FDLD signals of λ DNA in 1% agarose ($E=20$ V/cm). Application of the electric field corresponds to time zero.

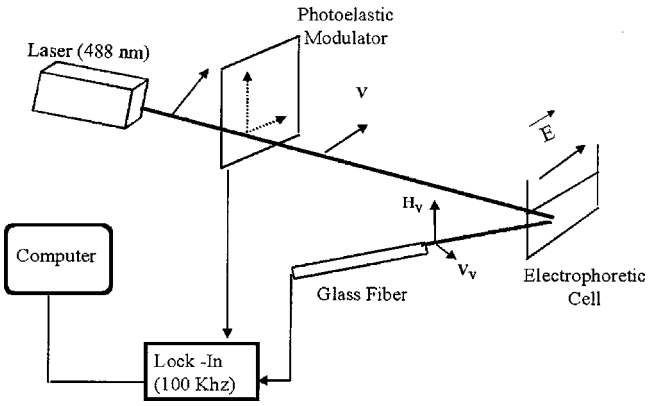

FIG. 5. Schematic diagram of the fluorescence polarization setup.

$$V_V \propto \tfrac{1}{8}\langle \sin^4\theta_s\rangle(1+2\cos^2\psi)\sin^2\chi' + \tfrac{1}{2}(\langle \sin^2\theta_s\rangle - \langle \sin^4\theta_s\rangle)\cos^2\chi', \tag{12}$$

$$V_H \propto [\tfrac{1}{4}\langle \sin^2\theta_s\rangle - \tfrac{1}{16}\langle \sin^4\theta_s\rangle(1+2\cos^2\psi)]\sin^2\chi' + [\tfrac{1}{2} - \tfrac{3}{4}\langle \sin^2\theta_s\rangle + \tfrac{1}{4}\langle \sin^4\theta_s\rangle]\cos^2\chi', \tag{13}$$

$$H_{V(x)} = H_{V(y)} \propto [\tfrac{1}{4}\langle \sin^2\theta_s\rangle - \tfrac{1}{16}\langle \sin^4\theta_s\rangle \times (1+2\cos^2\psi)]\sin^2\chi' + \tfrac{1}{4}\langle \sin^4\theta_s\rangle\cos^2\chi', \tag{14}$$

$$H_{H(x)} \propto [\tfrac{1}{2}(1-\langle \sin^2\theta_s\rangle) + (1+2\cos^2\psi)(-\tfrac{1}{8} + \tfrac{1}{8}\langle \sin^2\theta_s\rangle + \tfrac{1}{64}\langle \sin^4\theta_s\rangle)]\sin^2\chi' + (\tfrac{1}{4}\langle \sin^2\theta_s\rangle - \tfrac{1}{16}\langle \sin^4\theta_s\rangle)\cos^2\chi', \tag{15}$$

$$H_{H(y)} \propto [(1+2\cos^2\psi)(\tfrac{1}{8} - \tfrac{1}{8}\langle \sin^2\theta_s\rangle + \tfrac{3}{64}\langle \sin^4\theta_s\rangle)]\sin^2\chi' + (\tfrac{1}{4}\langle \sin^2\theta_s\rangle - \tfrac{3}{16}\langle \sin^4\theta_s\rangle)\cos^2\chi'. \tag{16}$$

Two main results arise from relations (12)–(16).

(i) Since H_H in a direction making an angle β with Ox in the xy plane is

$$H_H(\beta) = H_{Hx}\cos^2\beta + H_{Hy}\sin^2\beta, \tag{17}$$

the difference between $H_{H(x)}$ and $H_{H(y)}$ demonstrates the change in the angular distribution of fluorescence mentioned above.

(ii) From Eqs. (12) and (14) it is seen that χ', ψ, and $\langle \sin^4\theta\rangle$ are eliminated from the sum $V_V + 2H_V$, and that

$$V_V + 2H_V \propto \tfrac{1}{2}\langle \sin^2\theta_s\rangle(\cos^2\chi' + \sin^2\chi') = \tfrac{1}{2}\langle \sin^2\theta_s\rangle. \tag{18}$$

In the absence of an applied electric field, the orientation of the molecules is isotropic and thus $\langle \sin^2\theta_{s(E=0)}\rangle = \frac{2}{3}$ and $(V_V + 2H_V)_{(E=0)}$ is proportional to $\frac{1}{3}$. Therefore f can easily be calculated from

$$\frac{(V_V + 2H_V)_{(E)}}{(V_V + 2H_V)_{(E=0)}} = \tfrac{3}{2}\langle \sin^2\theta_s\rangle = 1 - f. \tag{19}$$

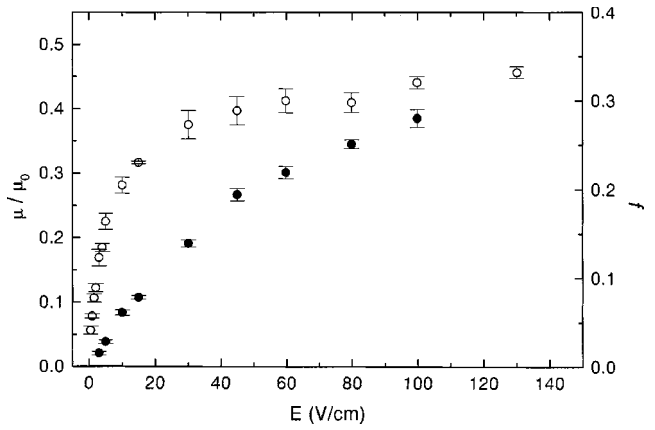

FIG. 6. Field dependence of mobility μ (○) and orientational factor f (●) for λ DNA in 1% agarose gel.

2. The fluorescence polarization setup

The experimental setup is depicted in Fig. 5. The additional elements are mounted on the same optical bench and use the same laser beam, with a vertical polarization, as for FRAP. By placing the photoelastic modulator, operating at 50 kHz, with its axis at 45°, the polarization of the incident beam oscillates between the vertical and horizontal directions. A first polarizer selecting the vertical polarization is placed before the cell, which therefore receives vertically polarized light, modulated at 100 kHz. A second polarizer, placed after the cell at the entrance of the collecting fiber, selects either the vertical (V_V) or horizontal (H_V) component of the fluorescence. The signal is demodulated by lock-in detection at 100 kHz and acquired with a computer.

IV. RESULTS AND DISCUSSION

Typical results for λ DNA in 1% agarose gel are depicted in Figs. 4 and 6. Figure 4 demonstrates the simultaneous recording of FRAP and FDLD. Of special relevance is the buildup of the FDLD signal with an overshoot at t_{ov} and an undershoot at t_u, as already reported by several groups. The field dependences of t_{ov} and of t_u are given in Table I, together with the velocity calculated from the fit of the FRAP signal to Eq. (2).

Figure 6 shows the field dependence of $\mu = v/E$ obtained from FRAP and of f as obtained from fluorescence polariza-

TABLE I. Characterization of the cyclic behavior ($L_p = 50$ nm; $L_{t_0} = 1080$ nm; $L_c = 16.5\,\mu$m; $\mu_0 = 3.2\times10^{-8}$ m^2 V^{-1} s^{-1}; $a = 490$ nm).

E (V/cm)	t_{ov} (s)	t_u (s)	v (μm s^{-1})	$\frac{(L)}{L_c}$	$\frac{\mu_0 E t_{ov}}{2L_c}$	$\frac{t_u}{t_{ov}}$	$\frac{\mu}{\mu_0}$
6.8	1.1	2.2	5.4	0.72	0.66	2.0	0.25
9.6	0.89	1.49	8.3	0.75	0.83	1.7	0.27
15	0.43	0.81	15.4	0.76	0.63	1.9	0.32
20	0.32	0.62	21.8	0.82	0.62	1.9	0.34
25.5	0.25	0.46	30.4	0.85	0.62	1.8	0.37
40	0.13	0.27	52.5	0.86	0.50	2.1	0.41
60	0.11	0.19	80.6	0.93	0.64	1.7	0.42

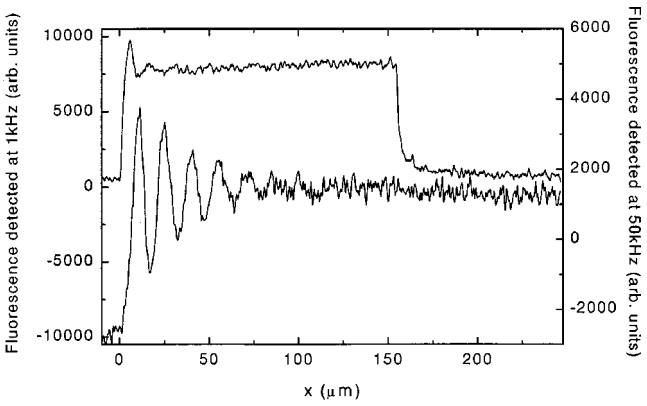

FIG. 7. Figure 4 redrawn as a function of the length covered by the molecules.

tion measurements. The most noticeable feature is the fact that μ tends to a limiting value at moderate fields ($\sim$50 V/cm) while f continues to increase.

We base our discussion of these results on the current description of DNA electrophoretic transport, called geometration, first proposed from computer simulation [21,22] and directly observed by fluorescence microscopy [23,24]. Each molecule is shown to oscillate during its motion between compact and elongated conformations. At fields where the tube, or set of pores containing one DNA molecule, can be considered as fully aligned with the field and the mobility reaches a limiting value, the cyclic process has been quantitatively decomposed by Popelka *et al.* [25] into the three following phases: ''in the first phase (duration t_1), the molecule in a random coil conformation encounters an obstacle and gets hooked. The two arms start to move at the same time in the direction of the electric field, leading to a U conformation of total tube length L_t. In the second phase (duration t_2) the chain starts to slide around the obstacle, the longer arm drags the shorter arm in a J conformation. In the third phase (duration t_3) the chain is released from the obstacle. The tension disappears and the extended I conformation moves while partly relaxing till it rapidly collides with a new obstacle, contracts back to a random coil, and starts a new cycle.''

A. Information from the simultaneous recording of μ, t_{ov}, and t_u

Åkerman [26] has proposed that the cyclic process can be characterized by its average period $\langle T\rangle$ and average step length $\langle L\rangle$ and has shown that $\langle T\rangle \sim t_u$. $\langle L\rangle$ can therefore be measured directly on Fig. 7 where the time scale of Fig. 4 has been transformed to a length scale using the average value $\langle v\rangle$ taken from the fit of the FRAP signal according to relation (2). $\langle L\rangle$ should then be compared to two limiting lengths: the original tube length L_{t_0} and the DNA contour length L_c. L_{t_0} can be calculated from the DNA mobility at vanishingly low fields, $\mu_{E\to 0}$, which provides the number N of ''blobs'' or pores occupied by a nonoverstretched DNA molecule:

$$\frac{\mu_{E\to 0}}{\mu_0}=\frac{1}{3N},\quad Na^2=2L_pL_c,\quad L_{t_0}=Na, \tag{20}$$

where L_p is the DNA persistence length and μ_0 the free solution mobility of DNA [27]. The corresponding values are given in Table I. A clear result is that $\langle L\rangle$ becomes comparable to L_c at fields of the order of 40 V/cm.

t_{ov} varies with $E^{-1.2\pm 0.1}$ as already noted [12] and $t_u/t_{ov}\cong 1.9$ in fair agreement with the value reported by Åkerman. t_{ov} can be compared to either the time needed to form the U conformation with arms of similar lengths, which is the most stable, $t_1=L_t/\mu_0 E$, or to the time where the U and J conformations disengage from the obstacle, i.e., $\langle T\rangle - t_3 = \langle T\rangle - L_t/v_0 = t_u - L_t/\mu_0 E$. One has therefore $t_u/t_{ov} = \mu_0/\mu$ or $1/1-\mu/\mu_0$. Since μ/μ_0 tends to a value $\sim$0.5 at high fields, both expressions give $t_u/t_{ov}\cong 2$ in fair agreement with the experiments.

B. Information from the parallel measurements of μ from FRAP and f from fluorescence polarization

The field dependence of μ and f in the steady-state regime substantiates the preceding considerations and permits one to obtain more detailed information from the existence of a limiting value of μ above 50 V/cm and the continuing rise of f above 50 V/cm.

The limiting value of $\mu/\mu_0\cong 0.45$ is very close to the prediction of [25] ($\mu/\mu_0=\frac{4}{9}$), based on the three-phase model, where the tube length is taken as constant on average and the arms extend in the field with a mobility μ_0, the resultant mobility μ being linked with the different motions of the center of mass during the three phases associated with U, J, and I conformations. Overstretching does not enter into the model since the friction factor in electrophoresis is proportional to the DNA contour length and not to the tube length, the hydrodynamic interactions being screened by the motion of the counterions [28].

It does, however, enter the value of f through the factor $a/l=L_t/L_c$ which changes from $2L_p/a$ for no overstretching to $a/l=1$ for full overstretching to the contour length. What we measured, however, is the time-weighted average over the oriented overstretched conformations and the unoriented coil conformation. What is observed is a value of $f\sim 0.20$ at 50 V/cm, where μ reaches a limiting high field value (full orientation of the tube), and $f\sim 0.28$ at 100 V/cm. From relation (11) these values give $F(2L_p/a)\cong 0.04$, $(L_t/L_c)_{50\ \mathrm{V/cm}}=0.54$, and $(L_t/L_c)_{100\ \mathrm{V/cm}}=0.63$. The fact that values of f larger than 0.04 are measured at fields $\approx$10 V/cm reveals that overstretching dominates the value of f long before full tube orientation. This has already been deduced from an analysis of the decay of birefringence [11,12]. The decay of FDLD in Fig. 4 clearly presents a fast initial decrease corresponding to the relaxation of the overstretching and a slow one corresponding to the reptation of the relaxed chain outside the oriented tube. Considering the signal to noise ratio, it is clear that continuing this analysis of the decay of the FDLD signal would require an averaging over a large number of pulses. It would also give the time constant of the long exponential, which is the reptation time. This has been measured by birefringence [29]. For λ DNA in 1% agarose $\tau_r\sim 6$ s, which seems slightly longer than would be deduced from the signal of Fig. 4. One should recall, however, that this time, as well as the values of μ, is very sensitive to the distribution of pore sizes, which seems to

depend on the preparation conditions of the gel (temperature of dissolution, cooling rate, etc.). That is another reason to perform simultaneous measurements.

V. CONCLUSION

Developing simultaneous measurements of the orientation and transport parameters (mobility, diffusion) on a FRAP setup equipped with fluorescence detected linear dichroism and polarization of fluorescence results in a very promising tool which will also be useful in various applications such as understanding DNA electrophoresis in solutions of hydrophilic polymers much below the overlap concentration [30] and studying the coupling of transport and flow of polymers near a wall [31]. For the purpose of this paper we have illustrated some of the capabilities of this tool by performing a computerized acquisition of several characteristics of the cyclic mechanism of DNA electrophoretic transport: the average mobility and cycle time t_u, the overshoot time t_{ov} corresponding to the first phase of the arm extension around an obstacle, and the average orientation of a segment over one cycle, which combined with an analysis of the FDLD decay can allow separation of the tube orientation and of overstretching of the tube length. The application of the method to DNA of varying lengths in agarose gels of varying concentrations will be the subject of a forthcoming paper.

[1] A. Ogston, Trans. Faraday Soc. **54**, 1754 (1958).
[2] P. J. D. Gennes, J. Chem. Phys. **55**, 572 (1971).
[3] L. S. Lerman and H. L. Frisch, Biopolymers **21**, 1754 (1982).
[4] O. J. Lumpkin, P. Déjardin, and B. H. Zimm, Biopolymers **24**, 1573 (1985).
[5] G. W. Slater and J. Noolandi, Biopolymers **24**, 2181 (1985).
[6] T. A. Duke, J. L. Viovy, and A. N. Semenov, Biopolymers **34**, 239 (1994).
[7] I. Hurley, Biopolymers **25**, 539 (1986).
[8] G. Holzwarth, K. V. Platt, C. B. M. Kee, R. W. Whitcomb, and G. D. Crater, Biopolymers **28**, 1043 (1989).
[9] K. V. Platt and G. Holzwarth, Phys. Rev. A **40**, 7292 (1989).
[10] M. Jonsson and B. Åkerman, Biopolymers **27**, 381 (1988).
[11] P. Mayer, J. Sturm, and G. Weill, Biopolymers **33**, 1347 (1993).
[12] P. Mayer, J. Sturm, and G. Weill, Biopolymers **33**, 1359 (1993).
[13] J. Davoust, P. F. Devaux, and L. Leger, EMBO J. **1**, 1233 (1982).
[14] B. Tinland, Electrophoresis **17**, 1519 (1996).
[15] B. Tinland, N. Pernodet, and A. Pluen, Biopolymers **46**, 201 (1998).
[16] L. Meistermann and B. Tinland, Phys. Rev. E **58**, 4801 (1998).
[17] W. Kuhn and F. Grün, Kolloid-Z. **101**, 248 (1942).
[18] G. Holzwarth, C. B. M. Kee, S. Steiger, and G. D. Crater, Nucleic Acids Res. **15**, 10 031 (1987).
[19] B. Åkerman, M. Jonsson, B. Norden, and M. Lalande, Biopolymers **28**, 1541 (1989).
[20] G. Weill and J. Sturm, Biopolymers **14**, 2537 (1975).
[21] J. M. Deutsch, Phys. Rev. Lett. **59**, 1255 (1987).
[22] J. M. Deutsch and T. L. Madden, J. Chem. Phys. **90**, 2476 (1989).
[23] D. Schwartz and M. Koval, Nature (London) **338**, 520 (1989).
[24] S. Smith, P. Aldridge, and J. Callis, Science **248**, 1221 (1989).
[25] S. Popelka, Z. Kabatek, J. L. Viovy, and B. Gas, J. Chromatogr., A **838**, 45 (1999).
[26] B. Åkerman, Electrophoresis **17**, 1027 (1996).
[27] B. Tinland, N. Pernodet, and G. Weill, Electrophoresis **17**, 1046 (1996).
[28] M. Doi and S. F. Edwards, *The Theory of Polymer Dynamics* (Oxford Science Publications, Oxford, 1986).
[29] J. Sturm and G. Weill, Phys. Rev. Lett. **62**, 1484 (1989).
[30] K. Starchev, J. Sturm, and G. Weill, Macromolecules **32**, 348 (1999).
[31] L. Leger, H. Hervet, G. Massey, and E. Durliat, J. Phys.: Condens. Matter **9**, 7719 (1997).